Available online at www.sciencedirect.com
ScienceDirect
Optics & Laser Technology 39 (2007) 1125–1129
Optics & Laser Technology
www.elsevier.com/locate/optlastec

Super-parallel holographic correlator with optical fixing

Dongdong Teng[a], Biao Wang[a,b,*], Tao Geng[a], Furi Ling Fu[b]

[a]*Electro-Optics Technology Center, Harbin Institute of Technology, Harbin 150001, PR China*
[b]*Institute of Optoelectronic and Composite Materials, School of Physics and Engineering, Sun Yat-sen University, Guangzhou 510275, PR China*

Received 12 October 2005; received in revised form 7 September 2006; accepted 8 September 2006
Available online 23 October 2006

Abstract

Seven thousand five hundred holograms are stored in 15 locations within a bar of Zn:Mn:Fe:$LiNbO_3$, using a signal beam that propagates along the long axis of the bar. At each location, angular multiplexing is performed with the reference light changing its orientation in two-dimensional space. The same angular multiplexing is repeated at different locations along the long axis of the Zn:Mn:Fe:$LiNbO_3$ bar. When operating as a holographic correlator, an input image is compared simultaneously with the records stored in all locations within the bar and is recalled accurately.

Keywords: Holographic correlator; Zn:Mn:Fe:$LiNbO_3$; Two-center recording

1. Introduction

Volume holographic correlators have been investigated extensively due to their inherent parallel processing ability which allows an input image to be compared simultaneously with all stored images [1–3]. The number of images that may be stored at one single location using angular multiplexing is limited [4]. However, while the combination of angular multiplexing with spatial multiplexing may be used to solve this problem, the requirement to move the recording medium to access the different spatial storage locations would influence the recognition rate, and fails to use the parallel processing capability efficiently.

Shahriar [5] developed a super-parallel holographic correlator by use of a holographic multiplexer–demultiplexer. This is a sophisticated system and requires the use of a high-power laser. In this paper, a new super-parallel holographic correlator with much simpler optical system is discussed. Crystals of doped $LiNbO_3$ are used as the recording medium. For the practical demonstration of the system, the two-center recording technique [6–8] is used for nonvolatile holographic storage.

2. Hologram recording and analysis

As shown in Fig. 1, holograms are recorded with a 90° geometry. The recording medium is shaped into a bar. The square head face acts as the incident face for the signal light. The reference light is incident from a rectangular side, approximately perpendicular to the signal light. The *c*-axis of the medium is oriented at 45° to these two incident faces. Angular multiplexing is performed using a rotation stage and the posterior 4-f system. Simultaneously, the rotation stage and the 4-f system, as a whole, may travel parallel with the long axis of the $LiNbO_3$ bar to implement spatial multiplexing.

For two-center recording, the recording medium is exposed to UV light before and during the recording of the holograms. Once the hologram recording process has been completed at one location, the UV illumination should be immediately blocked.

In our architecture, the signal light needs to propagate a rather long distance in the recording medium. Thus the light-induced scattering is a significant issue when the signal light exits the recording medium. Crystals of Zn:Fe:Mn:$LiNbO_3$(0.005 wt%ZnO, 0.075 wt% Fe_2O_3, 0.01 wt%MnO) and Fe:Mn:$LiNbO_3$(0.075 wt% Fe_2O_3, 0.01 wt%MnO) were grown to study the influence of Zn^{2+} on the light-induced scattering. The output from a He–Ne laser operating at 633 nm, with intensity

*Corresponding author. Electro-Optics Technology Center, Harbin Institute of Technology, Harbin 150001, PR China.
Tel./fax: +86 02084113293.
E-mail address: madiantengdong@163.com (D. Teng).

0030-3992/$ - see front matter © 2006 Elsevier Ltd. All rights reserved.
doi:10.1016/j.optlastec.2006.09.009

300 mW/cm^2, propagated along the long axis of the bar. The exit patterns observed after 60 s are shown in Fig. 2. It demonstrates that the doping of Zn plays effective role in reducing the scattering.

To facilitate angular multiplexing for one-center hologram recording, a recording schedule to achieve equal diffraction efficiencies has been reported previously, which assumed that the recording and erasure curves are both nonexponential [9]. However, for the technique used in this paper, the erasure curve is near-biexponential for two-center recording with UV (short wavelength) and recording light (long wavelength) simultaneously illuminating the bar. The recording and erasure curves can be approximated by

$$\sqrt{\eta} = A_0[1 - \exp(-t/\tau_r)], \tag{1}$$

$$\sqrt{\eta} = A\,\exp(-t/\tau_{e1}) + B\,\exp(-t/\tau_{e2}), \tag{2}$$

where τ_r is the recording time constant, τ_{e1} is the erasure time constant due to the recording wavelength and τ_{e2} is erasure time constant due to the UV illumination. For the final nonvolatile diffraction efficiency, we only consider the optical grating arising from the distribution of carriers stored in deep traps which are insensitive to the recording light. Only τ_{e2} is taken into account for the recording schedule. According to A. Adibi's study [10], with M holograms stored at one location, the exposure time of the nth hologram, t_n, is given by

$$t_n = \frac{\tau_{e2}}{n + \tau_{\tau 2}/t_1 - 1}. \tag{3}$$

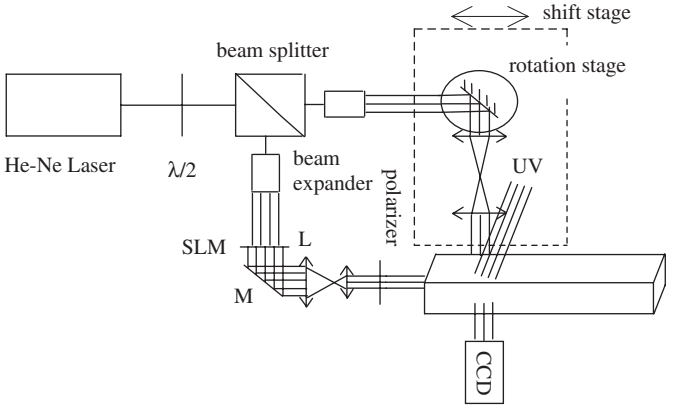

Fig. 1. Experimental configuration for spatial and angular multiplexing.

These recording and erasure time constants may be measured through a series of recording and erasure experiments with both the UV and the recording illumination on. In contrast to the situation in Ref. [10], the intensity of the long wavelength illumination for erasure is equal to the sum of reference and signal light' intensities for recording.

To achieve the spatial multiplexing, the reference light intensity $R_0\exp(-\alpha x)$ is the same for all locations, but the signal light intensity $S_0\exp(-\alpha z)$ is a function of position along the bar as shown in Fig. 3. The perturbation of the dielectric constant is denoted as

$$\Delta\varepsilon(x,z) \propto \frac{2R_0S_0\,\exp[-a(x+z)]}{R_0^2\,\exp(-2ax) + S_0^2\,\exp(-2az)}. \tag{4}$$

During the subsequent use of the hologram for correlation-based recognition, the incident signal light is also of intensity $S_0\exp(-\alpha z)$. The diffracted wave, proportional to $\Delta\varepsilon(x, z)$, propagates along the path of reference light. Thus the power of the diffracted wave received by the CCD can be expressed as

$$\sqrt{W_{out}} \propto 2R_0S_0^2 \int_V \frac{\exp[-a(D+2z)]}{R_0^2\,\exp(-2ax) + S_0^2\,\exp(-2az)}\,dV, \tag{5}$$

where D is the width of recording medium along the reference light and V the volume occupied by the grating.

Another influence of absorption is that the recording time constant varies for the different locations. According to Ref. [11], the dependence of the recording time constant

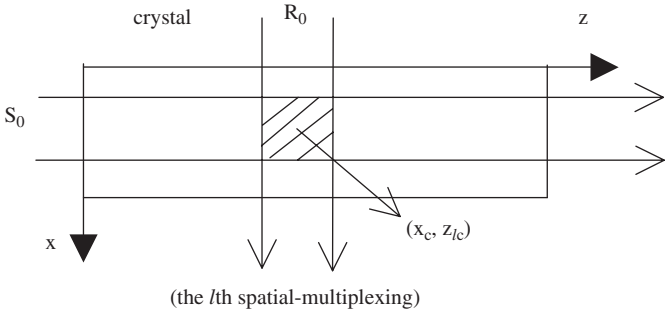

Fig. 3. Spatial multiplexing.

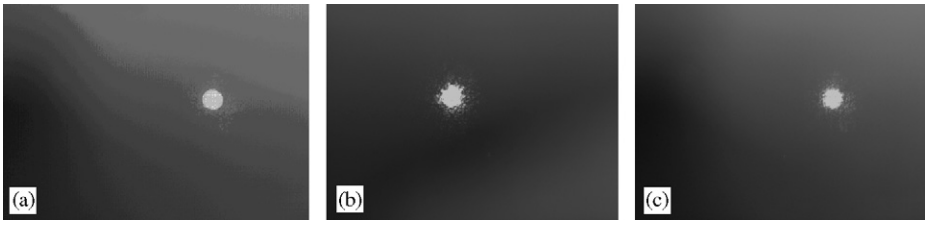

Fig. 2. Patterns of the emergent light after 60 s' illumination. (a) Weaken original light. (b) From Mn:Fe:$LiNbO_3$ bar of 40 mm.(c) From Zn:Mn:Fe:$LiNbO_3$ bar of 60 mm.

on the absorption can be denoted as

$$\tau_r(x,z) = \tau_r(0,0)\frac{R_0^2 + S_0^2}{R_0^2 \exp(-2ax) + S_0^2 \exp(-2az)}, \quad (6)$$

where $\tau_r(x, z)$ is the recording time constant at point of (x, z). Thus once the recording time constant of one point has been determined experimentally, that of different points may be calculated. As to τ_{e2}, because the UV light is same for all locations, it is taken as a constant.

At each location, the UV illumination is blocked after the hologram recording at that location is completed. During the recording of holograms at the other locations, the grating stored at this location is subsequently only exposed to signal light. Thus the final nonvolatile diffraction efficiency is not influenced by the hologram recording at the other locations. To ensure the power of the light diffracted from the different locations is equal, the exposure time of the last hologram recorded at each location should be different. In the following calculation, the storage unit for the lth spatial multiplexing is replaced by the center point of this storage unit, (x_c, z_{lc}). As shown in Fig. 2, the x_c is constant. One hologram is stored in the storage unit of (x_c, z_{lc}) with a exposure time, t_{lM}, that is sufficient for subsequent correlation-based recognition. This t_{lM} is the t_M in Eq. (3) for the lth spatial multiplexing. Combining Eqs. (1) and (5), one can set

$$K = \frac{R_0 S_0^2 \exp[-a(W + 2z_{lc})]}{R_0^2 \exp(-2ax_c) + S_0^2 \exp(-2az_{lc})} \times [1 - \exp(-t_{lM}/\tau_{lr})], \quad (7)$$

where τ_{lr} is the recording time constant of the point of (x_c, z_{lc}). Then t_{kM} can be determined by replacing z_{kc} and τ_{kc} of Eq. (7) by z_{lc} and τ_{lr}. Using Eq. (3), the recording schedule for angular-multiplexing of the kth location could be derived.

3. Experiment

We perform the super-parallel holographic correlator within a Zn:Mn:Fe:$LiNbO_3$ bar($2\alpha = 0.2\,cm^{-1}$) of $8\,mm \times 8\,mm \times 60\,mm$. Along the long axis, the bar is separated into 15 locations of equal length for spatial multiplexing. UV light is derived from a 100-W mercury lamp (wavelength, 404 nm, unpolarized; intensity, $25\,mW/cm^2$, homogeneous) and the recording light from a 150-mW He–Ne laser (wavelength, 633 nm, ordinary polarization; $1/e^2$ beam diameter, 3.0 mm). The crystal is pre-exposed to UV illumination for 50 min.

The patterns for storage consists of a the images of a series of buildings, which have had their edges enhanced by a second-order Laplacian edging operation. Examples are shown in Fig. 4. We calculated an algorithm to ensure that the transmitted light energy of each image is equal. The intensities of reference and signal light before entering the holographic medium are both $300\,mW/cm^2$.

At the first location of $z_{1c} = 2\,mm$ and $x_c = 4\,mm$, the recording and erasure experiment were repeated four times with both the UV and the recording illumination on. The recording and erasure curves are shown in Fig. 5. From this

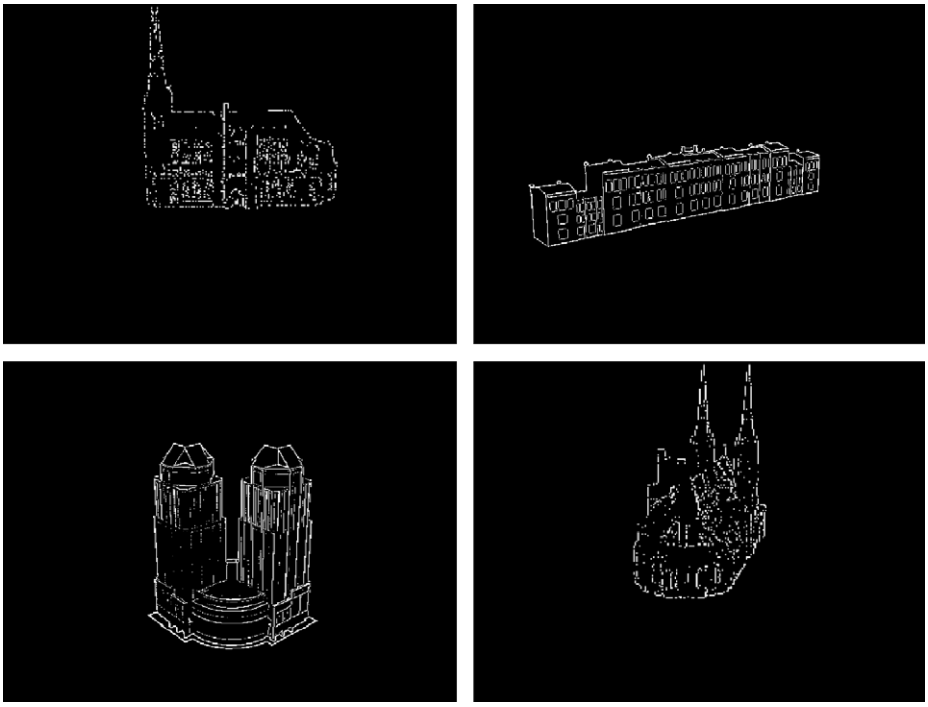

Fig. 4. Patterns for storage.

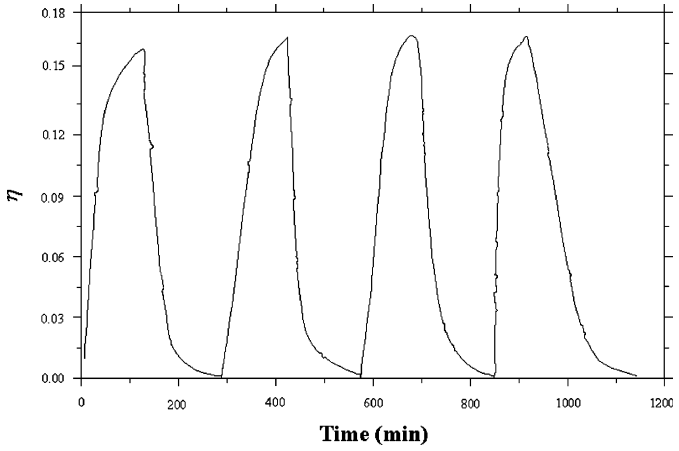

Fig. 5. Four cycles of recording and erasure with both UV and recording illumination on at the first location.

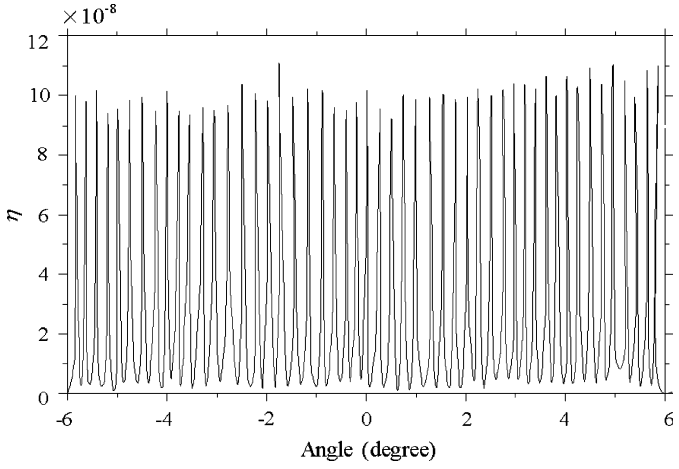

Fig. 6. Nonvolatile diffraction efficiencies at the first location.

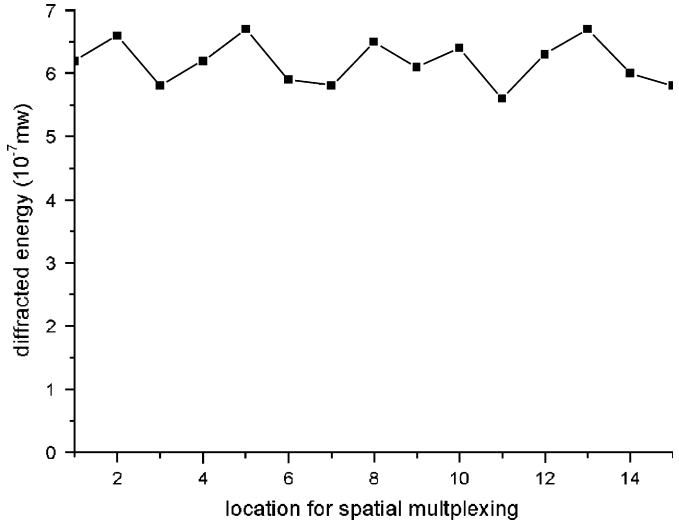

Fig. 7. Energy diffracted from different locations.

data it is possible to determine the recording and erasure time constants, $\tau_{1r} = 2840 \pm 250\,\mathrm{s}$, $\tau_{1e1} = 420 \pm 50\,\mathrm{s}$ and $\tau_{e2} = 4130 \pm 160\,\mathrm{s}$.

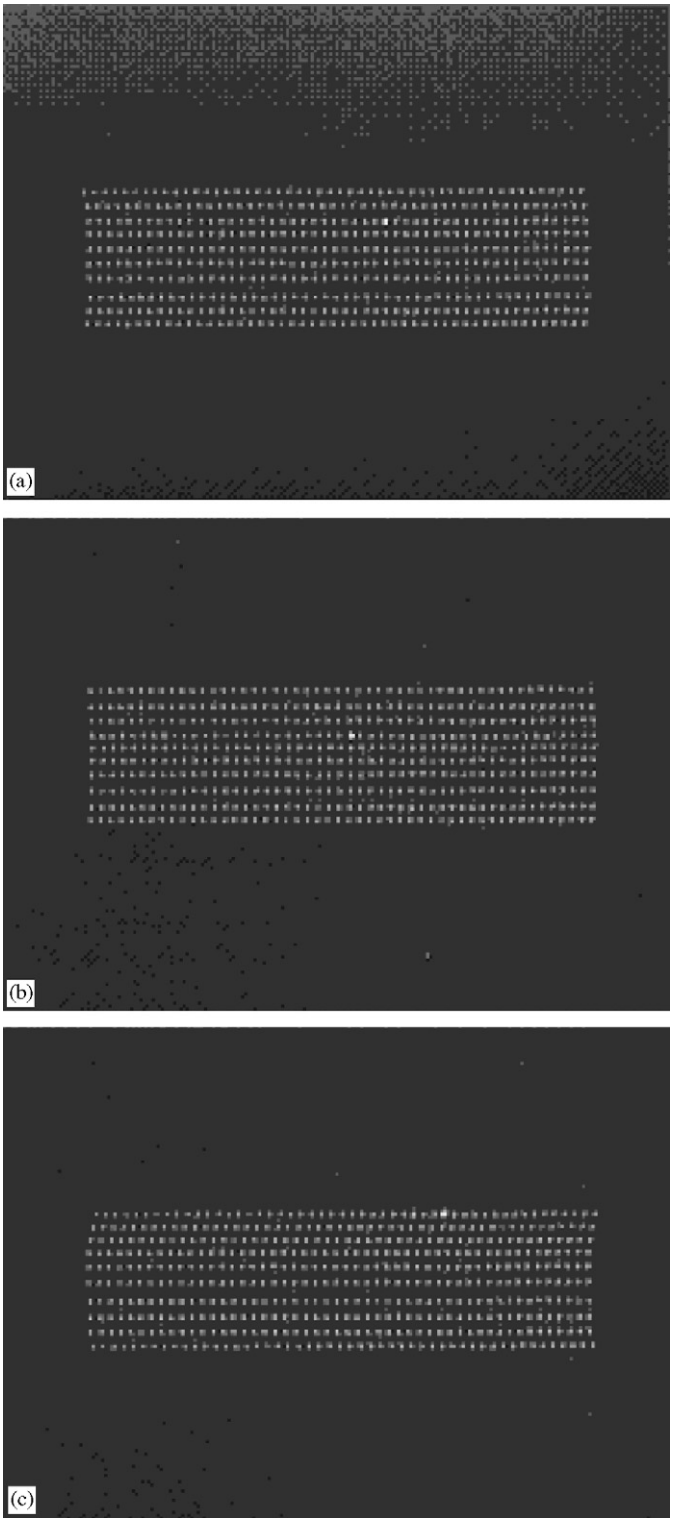

Fig. 8. Correlation peak patterns. (a) The first location. (b) The eighth location. (c) The last location.

For the first location, we take $t_{1M} = 2\,\mathrm{s}$ experimentally. Based on Eq. (3), we stored 50 holograms with angular separation of 0.05° within the level plane which included reference and signal light. With the crystal exposed to UV light at 633 nm for two hours, the final nonvolatile

diffraction efficiencies are approximately equivalent as shown in Fig. 6.

By using Eq. (6), the recording time constants for all locations are determined using $\tau_{1r} = 2840 \pm 250$ s. The maximum value is $\tau_{15r} = 4327 \pm 400$ s. Then with Eq. (7), we could calculate the exposure time of the last hologram for each location using $t_{1M} = 2$ s. Among them the maximum value is $t_{15M} = 6$ s. The same pattern is stored in all these 15 location with reference light of the same incident angle. As shown in Fig. 7, the energy diffracted from each location is approximately equal.

Finally, we demonstrated the super-parallel holographic correlator with 7500 images stored in 15 locations. For each location, the two-dimensional angle multiplexing (50×10) was implemented. The angular interval was 0.05° within the level plane and 0.09° within the vertical plane which is perpendicular to the level plane. In order to avoid interference from other locations, different refracting prisms were placed close to each location to guide the light diffracted from these locations to different directions. Thus 15 CCD may be used to receive all the correlation peak patterns simultaneously and the parallel recognition of all these 7500 patterns were realized. Fig. 8 shows the correlation peak patterns diffracted from the first, eighth, and last location with a self-correlation peak in. As a result, we recognized the 7500 patterns accurately.

4. Conclusion

In conclusion, we have proposed a novel super-parallel holographic correlator with optical fixing. The influence of absorption is discussed and a practical super-parallel holographic correlator has been demonstrated.

References

[1] Burr GW, Kobras S, Hanssen H, Coufal H. Content-addressable data storage by use of volume holograms. Appl Opt 1999;38:6779.
[2] Gu C, Fu H, Lien JR. Correlation patterns and cross-talk noise in volume holographic optical correlators. J Opt Soc Am A 1995;12:861.
[3] Ouyang C, Cao L, He Q, Liao Y, Wu M, Jin G. Sidelobe suppression in volume holographic optical correlators by use of speckle modulation. Opt Lett 2003;28:1972.
[4] Burr GW, Jefferson C, Coufal H, Jurich M, Hoffnagle J, Macfarlane R, et al. Volume holographic data storage at an areal density of 250 gigapixels/in^2. Opt Lett 2001;26:444–6.
[5] Sshahriar M, Tripathi R, Kleinschmit M, Donoghue J, Weathers W, Huq M, et al. Superparallel holographic correlator for ultrafast database searches. Opt Lett 2003;28:525.
[6] Adibi A, Buse K, Psaltis D. Sensitivity improvement in two-center holographic recording. Opt Lett 2000;25:539.
[7] Hesselink L, Orlov SS, Liu A, Akella A, Lande D, Neurgaonkar RR. Photorefractive Materials for nonvolatile volume holographic data storage. Science 1998;282:1089.
[8] Liu D, Liu L, Zhou C, Ren L, Li G. Nonvolatile holograms in $LiNbO_3$:Fe:Cu by use of the bleaching effect. Appl Opt 2002;41:6809.
[9] Mok FH, Tackitt MC, Stoll HM. Storage of 500 high-resolution holograms in a $LiNbO_3$ crystal. Opt Lett 1991;16:605.
[10] Adibi A, Buse K, Psaltis D. Multiplexing holograms in $LiNbO_3$:Fe:Mn crystals. Opt Lett 1999;24:652.
[11] Maniloff ES, Johnson KM. Effect of scattering on the dynamics of holographic recording and erasure in photorefractive lithium niobate. J Appl Phys 1993;73:541.